Ultrafast carrier dynamics in an InAs/InGaAs quantum dots-in-a-well heterostructure

R. P. Prasankumar[1*], R. S. Attaluri[2], R. D. Averitt[1], J. Urayama[3], N. Weisse-Bernstein[2], P. Rotella[2], A. D. Stintz[2], S. Krishna[2], and A. J. Taylor[1]**

[1]Center for Integrated Nanotechnologies, Los Alamos National Laboratory, Los Alamos, New Mexico 87545
[2] Center for High Technology Materials, EECE Department, University of New Mexico, Albuquerque, NM 87106
[3]Sandia National Laboratories, Albuquerque, NM 87106
**Corresponding author: rpprasan@lanl.gov*
***Current address: Department of Physics, Boston University, 590 Commonwealth Avenue, Boston, MA 02215*

Abstract: Ultrafast differential transmission spectroscopy is used to explore temperature-dependent carrier dynamics in an InAs/InGaAs quantum dots-in-a-well heterostructure. Electron-hole pairs are optically injected into the three dimensional GaAs barriers, after which we monitor carrier relaxation into the two dimensional InGaAs quantum wells and the zero dimensional InAs quantum dots by tuning the probe photon energy. We find that carrier capture and relaxation are dominated by Auger carrier-carrier scattering at low temperatures, with thermal emission playing an increasing role with temperature. Our experiments provide essential insight into carrier relaxation across multiple spatial dimensions.

OCIS codes: (320.7150) Ultrafast spectroscopy, (320.7130) Ultrafast processes in condensed matter, including semiconductors, (040.3060) Detectors, infrared, (040.5570) Quantum detectors, (230.5590) Quantum-well, -wire, and –dot devices

References and links

1. P. Bhattacharya, S. Ghosh, and A. D. Stiff-Roberts, "Quantum dot opto-electronic devices," Annu. Rev. Mater. Res. **34**, 1 (2004).
2. C. B. Murray, D. J. Norris, and M. G. Bawendi, "Synthesis and characterization of nearly monodisperse CdE (E=S, Se, Te) semiconductor nanocrystallites," J. Am. Chem. Soc. **115**, 8706 (1993).
3. S. Raghavan, P. Rotella, A. Stintz, B. Fuchs, S. Krishna, C. Morath, D. A. Cardimona, and S. W. Kennerly, "High-responsivity, normal-incidence long-wave infrared (λ~7.2 μm) InAs/$In_{0.15}Ga_{0.85}As$ dots-in-a-well detector," Appl. Phys. Lett. **81**, 1369 (2002).
4. G. T. Liu, A. Stintz, H. Li, T. C. Newell, A. L. Gray, P. M. Varangis, K. J. Malloy, and L. F. Lester, "The influence of quantum-well composition on the performance of quantum dot lasers using InAs/InGaAs dots-in-a-well (DWELL) structures," IEEE J. Quantum Elect. **36**, 1272 (2000).
5. J. Shah, *Ultrafast spectroscopy of semiconductors and semiconductor nanostructures* (Springer, New York, 1999).
6. V. I. Klimov, "Spectral and dynamical properties of multiexcitons in semiconductor nanocrystals," Annu. Rev. Phys. Chem. **58**, 635 (2007).
7. A. S. Lenihan, M. V. G. Dutt, D. G. Steel, P. Bhattacharya, and S. Ghosh, "Biexcitonic resonance in the nonlinear optical response of an InAs quantum dot ensemble," Phys. Rev. B **69**, 045306 (2004).
8. J. Urayama, T. B. Norris, J. Singh, and P. Bhattacharya, "Observation of phonon bottleneck in quantum dot electronic relaxation," Phys. Rev. Lett. **86**, 4930 (2001).
9. J. Urayama, T. B. Norris, H. Jiang, J. Singh, and P. Bhattacharya, "Differential transmission measurement of phonon bottleneck in self-assembled quantum dot intersubband relaxation," Physica B **316-317**, 74 (2002).
10. S. Krishna, "Quantum dots-in-a-well infrared photodetectors," J. Phys. D: Appl. Phys. **38**, 2142 (2005).
11. L. F. Lester, A. Stintz, H. Li, T. C. Newell, E. A. Pease, B. A. Fuchs, and K. J. Malloy, "Optical characteristics of 1.24-um InAs quantum-dot laser diodes," IEEE Photon. Technol. Lett. **11**, 991 (1999).
12. A. Fiore, P. Borri, W. Langbein, J. M. Hvam, U. Oesterle, R. Houdre, R. P. Stanley, and M. Ilegems, "Time-resolved optical characterization of InAs/InGaAs quantum dots emitting at 1.3 um," Appl. Phys. Lett. **76**, 3430 (2000).
13. F. Pulizzi, A. J. Kent, A. Patane, L. Eaves, and M. Henini, "Time-resolved photoluminescence of InAs quantum dots in a GaAs quantum well," Appl. Phys. Lett. **84**, 3046 (2004).

#90338 - $15.00 USD Received 30 Nov 2007; revised 18 Dec 2007; accepted 12 Jan 2008; published 15 Jan 2008

14. X. Mu, Y. J. Ding, B. S. Ooi, and M. Hopkinson, "Investigation of carrier dynamics on InAs quantum dots embedded in InGaAs/GaAs quantum wells based on time-resolved pump and probe differential photoluminescence," Appl. Phys. Lett. **89**, 181924 (2006).
15. A. I. Tartakovskii, R. S. Kolodka, H. Y. Liu, M. A. Migliorato, M. Hopkinson, M. N. Makhonin, D. J. Mowbray, and M. S. Skolnick, "Exciton fine structure splitting in dot-in-a-well structures," Appl. Phys. Lett. **88**, 131115 (2006).
16. G. Raino, G. Visimberga, A. Salhi, M. De Vittorio, A. Passaseo, R. Cingolani, and M. De Giorgi, "Simultaneous filling of InAs quantum dot states from the GaAs barrier under nonresonant excitation," Appl. Phys. Lett. **90**, 111907 (2007).
17. T. Piwonski, I. O'Driscoll, J. Houlihan, G. Huyet, R. J. Manning, and A. V. Uskov, "Carrier capture dynamics of InAs/GaAs quantum dots," Appl. Phys. Lett. **90**, 122108 (2007).
18. I. O'Driscoll, T. Piwonski, C.-F. Schleussner, J. Houlihan, G. Huyet, and R. J. Manning, "Electron and hole dynamics of InAs/GaAs quantum dot semiconductor optical amplifiers," Appl. Phys. Lett. **91**, 071111 (2007).
19. S. Krishna, S. Raghavan, G. von Winckel, P. Rotella, A. Stintz, C. P. Morath, D. Le, and S. W. Kennerly, "Two color InAs/InGaAs dots-in-a-well detector with background-limited performance at 91 K," Appl. Phys. Lett. **82**, 2574 (2003).
20. T. S. Sosnowski, T. B. Norris, H. Jiang, J. Singh, K. Kamath, and P. Bhattacharya, "Rapid carrier relaxation in In0.4Ga0.6As/GaAs quantum dots characterized by differential transmission spectroscopy," Phys. Rev. B **57**, R9423 (1998).
21. T. B. Norris, K. Kim, J. Urayama, Z. K. Wu, J. Singh, and P. Bhattacharya, "Density and temperature dependence of carrier dynamics in self-organized InGaAs quantum dots," J. Phys. D: Appl. Phys. **38**, 2077 (2005).
22. H. Jiang and J. Singh, "Strain distribution and electronic spectra of InAs/GaAs self-assembled dots: An eight-band study," Phys. Rev. B **56**, 4696 (1997).
23. A. L. Efros, V. A. Kharchenko, and M. Rosen, "Breaking the phonon bottleneck in nanometer quantum dots: role of Auger-like processes," Solid State Commun. **93**, 281 (1995).
24. V. I. Klimov, "Optical nonlinearities and ultrafast carrier dynamics in semiconductor nanocrystals," J. Phys. Chem. B **104**, 6112 (2000).
25. F. Quochi, M. Dinu, L. N. Pfeiffer, K. W. West, C. Kerbage, R. S. Windeler, and B. J. Eggleton, "Coulomb and carrier-activation dynamics of resonantly excited InAs/GaAs quantum dots in two-color pump-probe experiments," Phys. Rev. B **67**, 235323 (2003).
26. V. I. Klimov and D. W. McBranch, "Auger-process-induced charge separation in semiconductor nanocrystals," Phys. Rev. B **55**, 13173 (1997).
27. Y. Toda, O. Moriwaki, M. Nishioka, and Y. Arakawa, "Efficient carrier relaxation mechanism in InGaAs/GaAs self-assembled quantum dots based on the existence of continuum states," Phys. Rev. Lett. **82**, 4114 (1999).
28. U. Bockelmann and T. Egeler, "Electron relaxation in quantum dots by means of Auger processes," Phys. Rev. B **46**, 15574 (1992).
29. B. Ohnesorge, M. Albrecht, J. Oshinowo, A. Forchel, and Y. Arakawa, "Rapid carrier relaxation in self-assembled InxGa1-xAs/GaAs quantum dots," Phys. Rev. B **54**, 11532 (1996).
30. R. Ferreira and G. Bastard, "Unbound states in quantum heterostructures," Nanoscale Res. Lett. **1**, 120 (2006).
31. A. V. Uskov, J. McInerney, F. Adler, H. Schweizer, and M. H. Pilkuhn, "Auger carrier capture kinetics in self-assembled quantum dot structures," Appl. Phys. Lett. **72**, 58 (1998).
32. E. W. Bogaart, J. E. M. Haverkort, T. Mano, T. van Lippen, R. Notzel, and J. H. Wolter, "Role of the continuum background for carrier relaxation in InAs quantum dots," Phys. Rev. B **72**, 195301 (2005).
33. A. Vasanelli, R. Ferreira, and G. Bastard, "Continuous absorption background and decoherence in quantum dots," Phys. Rev. Lett. **89**, 216804 (2002).
34. R. Ferreira and G. Bastard, "Phonon-assisted capture and intradot Auger relaxation in quantum dots," Appl. Phys. Lett. **74**, 2818 (1999).
35. H. Jiang and J. Singh, "Radiative and non-radiative inter-subband transition in self-assembled quantum dots," Physica E **2**, 720 (1998).
36. J. Urayama, T. B. Norris, H. Jiang, J. Singh, and P. Bhattacharya, "Temperature-dependent carrier dynamics in self-assembled InGaAs quantum dots," Appl. Phys. Lett. **80**, 2162 (2002).
37. J. Siegert, S. Marcinkevicius, and Q. X. Zhao, "Carrier dynamics in modulation-doped InAs/GaAs quantum dots," Phys. Rev. B **72**, 085316 (2005).
38. Z.-K. Wu, H. Choi, X. Su, S. Chakrabarti, P. Bhattacharya, and T. B. Norris, "Ultrafast electronic dynamics in unipolar n-doped InGaAs-GaAs self-assembled quantum dots," IEEE J. Quantum Elect. **43**, 486 (2007).
39. H. Lim, S. Tsao, W. Zhang, and M. Razeghi, "High-performance InAs quantum-dot infrared photodetectors grown on InP substrate operating at room temperature," Appl. Phys. Lett. **90**, 131112 (2007).

#90338 - $15.00 USD Received 30 Nov 2007; revised 18 Dec 2007; accepted 12 Jan 2008; published 15 Jan 2008

1. Introduction

Low dimensional semiconductor nanostructures have attracted much attention due to the unique size-dependent scaling of their physical properties, providing researchers an opportunity to tune these parameters in a manner not afforded by naturally occurring bulk materials. The intriguing physics in these systems, along with their immense potential for applications in areas including electronics and photonics, has driven an intense research effort aimed at understanding and controlling their properties. The most heavily studied nanostructures are two dimensional (2D) quantum wells (QWs) and zero dimensional (0D) quantum dots (QDs) since high quality samples can be readily fabricated, most often through epitaxial self-assembly or colloidal chemistry [1, 2]. The unique optical characteristics of these nanosystems make them ideal for photonic applications including infrared photodetection [3] and semiconductor lasing [4]. However, in order to optimize device properties such as power consumption and modulation speed, a comprehensive understanding of non-equilibrium density and temperature dependent carrier dynamics in these nanostructures is vital. Therefore, an extensive body of research, dating back to the 1980s, has focused on a detailed characterization of carrier dynamics in QWs and QDs after pulsed optical excitation [5, 6], revealing unique features such as carrier multiplication [6], biexciton formation [6, 7], and a phonon bottleneck for carrier relaxation [8, 9]. Despite the intense effort in this area, very few time-resolved optical studies have been performed on heterostructures intentionally designed to display multiple degrees of spatial confinement. This is an important avenue of study, as combinations of two-dimensional, one-dimensional, and zero-dimensional nanostructures are beginning to find many photonic applications.

A well known example of this concept is the dots-in-a-well (DWELL) heterostructure, which combines quantum wells and quantum dots in an effort to overcome the limitations of conventional QW-and-QD-based photodetectors and lasers [10]. These restrictions include the inability of conventional quantum well infrared photodetectors (QWIPs) to operate at normal incidence, necessitating the fabrication of gratings and optocouplers in the device. Quantum-dot infrared photodetectors (QDIP) have also been used in a variety of settings, but are limited by thermal emission and difficulties in control of the operating wavelength. In addition, QW-and-QD-based lasers suffer from relatively high thresholds and low gain [4].

The DWELL design offers an appealing approach towards overcoming these limitations. These heterostructures, typically grown by molecular beam epitaxy (MBE), are based on InAs quantum dots placed in a thin InGaAs quantum well (QW) that is subsequently sandwiched between GaAs barrier layers [3, 10]. This lowers the ground state of the QD relative to the GaAs band edge, reducing thermal emission. By altering the thickness and composition of the InGaAs well surrounding the dots, the position of the excited state can be varied without changing the QD ground state, enabling control of the operating wavelength. Confinement of electrically injected carriers to a two dimensional QW also increases carrier capture by the QDs, reducing lasing thresholds and increasing the gain [4, 11]. These devices have also been incorporated into 320x256 and 640x512 focal plane arrays for thermal imaging applications [10]. The DWELL structure is especially promising for applications in quantum information since discrete dot levels are isolated from decoherence-inducing continuum states. However, further improvements in this technology will require ultrafast spectroscopic techniques to improve understanding of carrier relaxation and transport in these novel nanostructures.

In this work, we perform temperature and wavelength dependent differential transmission (DT) spectroscopy to examine carrier relaxation in a DWELL heterostructure. Although some time-resolved measurements have been performed on quantum dots-in-a-well structures [12-18], few have aimed at understanding the influence of multiple degrees of spatial confinement on carrier dynamics, and to the best of our knowledge these are the first pump-probe measurements of carrier relaxation in a DWELL heterostructure after photoexcitation of electron-hole pairs in the barriers. This allows us to temporally resolve carrier relaxation from the three dimensional (3D) barriers into 2D quantum well and 0D quantum dot states by tuning the probe wavelength. Our measurements demonstrate that carrier dynamics in the

#90338 - $15.00 USD Received 30 Nov 2007; revised 18 Dec 2007; accepted 12 Jan 2008; published 15 Jan 2008

DWELL system at the investigated densities are dominated by Auger-type carrier-carrier scattering, with electron-electron scattering governing electron capture from the QW into the QD excited state and electron-hole scattering efficiently relaxing electrons from the QD excited state to the QD ground state. At higher temperatures, we find that thermal emission plays a significant role, causing carriers to be distributed over many adjacent levels in the DWELL heterostructure. These experiments provide fundamental insight into carrier relaxation in a system designed to exhibit multidimensional quantum confinement, along with information relevant to optimizing performance in DWELL-based photodetectors and lasers.

2. Experimental results and discussion

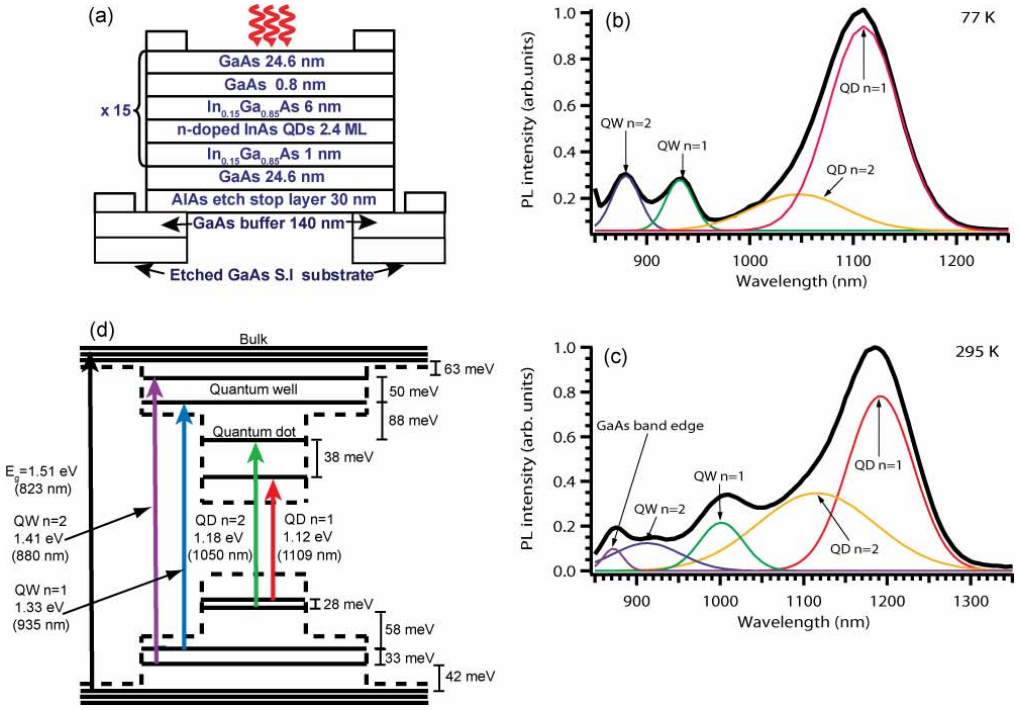

Fig. 1. (a). Schematic of the DWELL structure. (b). PL spectrum at 77 K. (c). PL spectrum at 295 K. (d). Energy level schematic at 77 K.

The DWELL device structure is depicted in Fig. 1(a). It is comprised of 15 layers, each consisting of 2.4 ML of InAs QDs (density~4.6×10^{10} cm^{-2}) grown on a 1 nm InGaAs QW, capped by a 6 nm InGaAs QW, and placed in a GaAs matrix; further growth details are described in references [3] and [19]. The QDs are doped with ~1 electron/dot for detector applications. The semi-insulating GaAs substrate was etched off to eliminate any influence on the measured signals.

Intensity-dependent photoluminescence (PL) experiments were performed to characterize the interband optical transitions in the DWELL heterostructure [20, 21]. Figure 1(b) depicts PL measurements taken on our DWELL sample at 77 K. Gaussian curve fits to the 77 K data reveal two QD interband transitions, with the QD excited (n=2) state centered at 1050 nm (1.18 eV) and the ground (n=1) state centered at 1109 nm (1.12 eV). The width of these peaks is due to inhomogeneous broadening of the dot size distribution. The QW n=2 and n=1 states are centered at 880 nm (1.41 eV) and 935 nm (1.33 eV), respectively. These interband transitions in the QDs and QWs are due to electron and hole levels that have the same quantum number n. There are also expected to be a large number of closely spaced "dark" hole levels that do not contribute to the interband optical transitions due to valence band degeneracy and the large effective mass of holes as compared to electrons [22, 23]. At 295 K [Fig. 1(c)], the PL peaks shift to longer wavelengths, as expected from the temperature

#90338 - $15.00 USD Received 30 Nov 2007; revised 18 Dec 2007; accepted 12 Jan 2008; published 15 Jan 2008

dependence of the bulk GaAs and InAs band gaps. The center wavelengths are 1115 nm (1.12 eV) and 1192 nm (1.04 eV) for the n=2 and n=1 transitions, respectively. The center wavelengths of the two lowest QW interband transitions are 912 nm (1.36 eV) and 1001 nm (1.24 eV). This allowed us to draw schematics of the DWELL energy levels at 77 K [Fig. 1(d)] and 295 K (not shown), assuming a 60:40 energy splitting between conduction and valence bands. The energy levels depicted in Fig. 1(d) are average values, as individual dots within the inhomogeneously broadened size distribution may have a different energy level structure.

Optical pump-probe experiments were based on a 100 kHz regeneratively amplified Ti:sapphire laser system producing 50 fs, 10 μJ pulses at 800 nm. The output beam is split into two equal parts to concurrently pump two optical parametric amplifiers (OPA). The visible OPA produces a signal beam tunable from 480-700 nm, an idler beam tunable from 930-2300 nm, and a residual pump beam at 400 nm. Similarly, the IR OPA produces a signal tunable from 1.1-1.6 μm and an idler tunable from 1.6-2.4 μm, with a residual pump at 800 nm. This enables measurements with independently tunable pump and probe wavelengths over a range of 400 nm (3.1 eV) to 3 μm (0.41 eV) and sub-100 fs time resolution.

Temperature-dependent differential transmission (DT) measurements were performed near normal incidence with a pump wavelength of 800 nm (1.55 eV) and fluence of 2.8 uJ/cm^2. This excites a carrier density of 1.8×10^{11} cm^{-2} in the GaAs barrier layers, corresponding to ~4 electron-hole pairs (ehp) per dot. The probe wavelength was tuned from 939-1250 nm (0.99-1.32 eV) at each temperature to track carrier relaxation in the DWELL heterostructure. This range of probe wavelengths allowed us to examine carrier capture and relaxation processes in the lowest QW (n=1) state and both QD states at low temperatures; at high temperatures the low energy side of the QW n=2 state also overlaps with the high energy side of our probe spectrum. It is worth noting that due to the relatively large size distribution of our QDs and broad bandwidth (~30 nm) of our probe pulses, the DT signal at certain probe wavelengths (particularly 1074 and 1103 nm) will have contributions from both QD n=1 and n=2 states. Therefore, when analyzing time dependent traces, we only consider probe wavelengths at which the contribution of the transition of interest to the DT signal is at least a factor of 5 greater than that of any other transition, as estimated from the measured PL spectra.

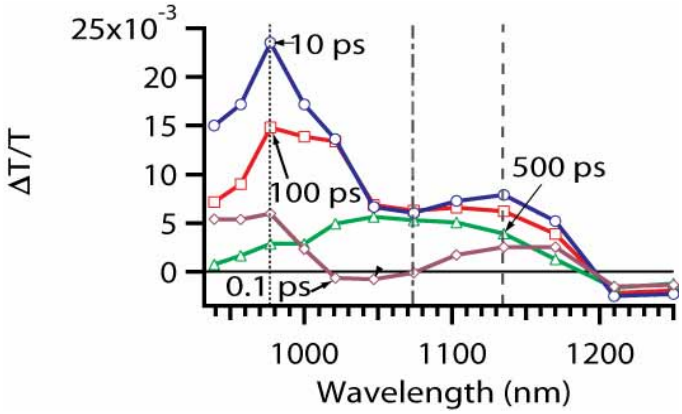

Fig. 2. Differential transmission spectrum taken at 30 K. The approximate positions of the QW n=1, QD n=2, and QD n=1 states are indicated by the dotted, dot-dashed, and dashed lines, respectively.

Figure 2 depicts the differential transmission spectrum for time delays of t=0.1, 10, 100, and 500 ps at 30 K. The DT signal is proportional to the sum of the electron and hole occupations of the QD levels [20]; therefore, our DT measurements can directly track the temporal evolution of carrier populations in the DWELL heterostructure. The peak positions indicated in the 30 K DT spectrum of Fig. 2 are red shifted from those obtained through PL

#90338 - $15.00 USD Received 30 Nov 2007; revised 18 Dec 2007; accepted 12 Jan 2008; published 15 Jan 2008

measurements [Fig. 1(b)], likely due to the significantly lower carrier density used in the DT experiments [20, 24, 25]. The DT signal at t=0.1 ps clearly shows that optically excited carriers rapidly populate the QW and QD n=1 states. However, this signal is negative for a band of wavelengths around the QD n=2 state (1021-1074 nm). Fluence-dependent measurements indicate that this negative signal increases in amplitude and persists for longer times with increasing excitation density (data not shown here). There is also a negative DT signal for long wavelengths (1200-1250 nm) which remains at long time delays, quite similar to that observed in ref. [20]. These negative signals are likely due to density-induced Coulomb level shifts [24, 25], although there may be contributions from surface/interface related trap states [26] or biexciton formation [6, 7]. We will discuss fluence-dependent dynamics in a future publication, focusing here on temperature-dependent dynamics at an excitation level of 4 ehp/dot, at which the energy level schematic depicted in Fig. 1(d) can reliably be used to interpret our data.

The "camel back" shaped DT spectrum reveals that all energy levels within the heterostructure are maximally populated by t=10 ps. From Fig. 2, it can be seen that the carriers leave the QW states on a time scale of a few hundred ps and are captured into the QDs, fully depopulating the QWs in ~500 ps. A particularly long relaxation is observed at the QD n=2 state, where curve fits indicate that the DT signal decays with a ~2.5 ns time constant. The DT signal at the ground state decays more rapidly, with a time constant of ~1 ns. More insight into carrier dynamics in the DWELL heterostructure can be obtained by examining the time dependence of the DT signal at different probe energies.

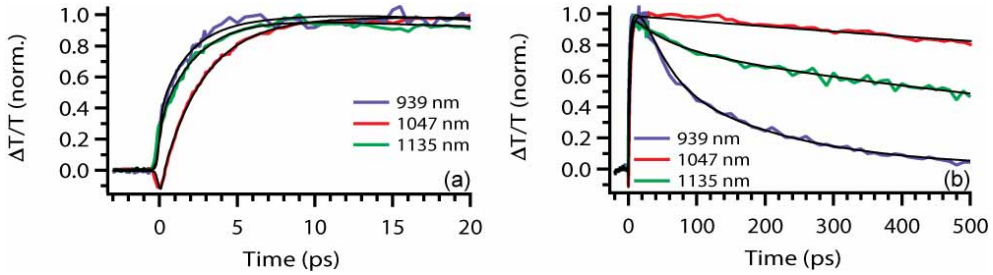

Fig. 3. Normalized 30 K time-dependent DT signals at the QW n=1 (977 nm) state, QD n=2 (1047 nm) and QD n=1 (1135 nm) states at (a) short and (b) long time delays.

Figure 3 depicts low temperature time-dependent DT traces at the QW n=1, QD n=2, and QD n=1 states at early (a) and late (b) times. By analyzing this data, we can discern the relative contributions of processes including relaxation through a finite continuum of states, carrier-phonon scattering, electron-electron scattering, and electron-hole scattering to carrier capture and relaxation within the DWELL heterostructure. We first compare the time-resolved DT traces at early times [Fig. 3(a)] to understand carrier capture dynamics. The rise times of these signals (~2-4 ps), due to carrier capture into QW and QD states, are comparable across the measured wavelength range, indicating that carriers are relaxing into the QD states at rates comparable with the relaxation into the lowest QW state. This contrasts with previous DT measurements on self-assembled InAs QDs at low excitation densities of <1 ehp/dot, in which a sequential relaxation of electrons from the n=2 to the n=1 state was observed [8, 21]. Our results do compare well with time-resolved PL measurements on a similar DWELL structure, in which the rise times of the PL signal from the QW and both QD states were ~6 ps [16]. This was attributed to carrier relaxation through a finite continuum of states, allowing carriers to rapidly populate QD states through phonon emission [27]. However, this is likely not the operative mechanism for QD carrier capture in our measurements, as will be demonstrated below.

Carrier capture into the QWs and QDs can instead be understood as follows: after photoexcitation in the GaAs barriers, electrons and holes are captured by the QW and quickly relax to the lowest QW state through phonon emission [5], bleaching it within ~2 ps as seen in

#90338 - $15.00 USD Received 30 Nov 2007; revised 18 Dec 2007; accepted 12 Jan 2008; published 15 Jan 2008

Fig. 3(a). The holes will simultaneously relax through the densely spaced valence band levels through LO and LA phonon emission, populating the lowest QD states on a sub-ps time scale [20]. This causes the initial rise in the DT signal at the QD excited and ground state energies.

The rise time of the QD n=2 signal [Fig. 3(a)] is also due to electron capture into the QDs, which is governed by Auger carrier-carrier scattering processes [28, 29]. According to refs. [28] and [30], efficient Auger relaxation will occur for photoexcited carrier densities greater than 10^{11} cm^{-2}. Both electron-electron scattering and electron-hole scattering are expected to influence the observed dynamics. However, for the carrier density used here (~$1.8x10^{11}$ cm^{-2}), electron-electron scattering rates are calculated to be approximately two orders of magnitude larger than electron-hole scattering rates [30, 31], allowing us to identify this as the main channel for QD electron capture. In this scenario, two electrons in the QW states will scatter via an Auger process, with one electron relaxing into the QD n=2 state and the other electron ejected to higher QW states. Electrons can also be directly captured to the QD n=1 state through Auger scattering [9], although the large energy separation between the QD n=1 state and the lowest QW state [Fig. 1(d)] makes it much less probable than capture to the QD n=2 state [30].

We can eliminate other possible avenues for QD carrier capture through examining the energy level schematic of Fig. 1(d) while also considering the temperature and fluence dependence of the QD n=2 rise time. The existence of a finite continuum of states, typically extending from the bulk band edge to below the QD n=2 state, has been suggested as a mechanism for fast carrier relaxation in certain quantum dot structures [16, 27, 32]. These continuum states are believed due to intrinsic crossed transitions between delocalized wetting layer/barrier states and bound QD states (e.g., from a GaAs valence band state to the QD n=1 conduction band state) [33]. Therefore, when two particles are located in a QD excited state with energy higher than a crossed transition, the bound state will autoionize, with the final state composed of one particle in a lower energy bound state and another particle ejected into the continuum [30, 33].

In our DWELL structure, the presence of the QW lowers the QD energy levels relative to the bulk band edge [3, 19]. Therefore, the crossed bound-continuum transitions have higher energies than the QD n=2 transition, unlike in many conventional self-assembled QD heterostructures [33]. The lowest energy DWELL bound-continuum transition is between the GaAs valence band and QD n=1 conduction band state, calculated from Fig. 1(d) to be at 970 nm (1.28 eV). This crossed transition has a higher energy than the 1.18 eV QD n=2 transition, making autoionization of the n=2 state unlikely. Relaxation through a finite continuum of states thus cannot explain the observed rapid carrier capture into the QDs in our DWELL heterostructure. However, we cannot rule out contributions from a crossed transition between the GaAs continuum valence band states and the QD n=1 conduction band state to the 977 nm peak in the DT spectrum at 30 K.

We can eliminate carrier-phonon scattering as a possible mechanism for the fast rise at the QD n=2 state by noting that the separation between the lowest QW state and n=2 QD state is ~88 meV, making electron capture into the QD through single phonon emission impossible and capture through multiphonon emission very unlikely for energy separations that are not an exact multiple of the LO phonon energy (ω_{LO}=32 meV for InAs) [34, 35]. Further support comes from noting that the rise times measured at all wavelengths do not depend significantly on temperature, which contradicts a phonon-assisted process [36]. This also backs the minimal role of relaxation through a finite continuum of states in QD carrier capture, as this process is also expected to be temperature-dependent [32]. Finally, our fluence-dependent data (not shown) is also consistent with an Auger scattering process, as it reveals a rise time that decreases with pump fluence at the QD excited state [29, 32]. We can therefore isolate electron-electron scattering as the mechanism for carrier capture into the QD n=2 state.

Electron relaxation from the QD n=2 state to the n=1 conduction band states, manifested in the rise time of the QD n=1 DT signal [Fig. 3(a)], occurs through electron-hole scattering. The ~38 meV separation between the QD n=2 and n=1 conduction band states suggests that carrier-phonon scattering is not significant at this temperature. Auger electron-electron

#90338 - $15.00 USD Received 30 Nov 2007; revised 18 Dec 2007; accepted 12 Jan 2008; published 15 Jan 2008

scattering does not conserve energy for this process, due to the lack of nearby continuum states for an electron to scatter into [Fig. 1(d)]. However, the holes can easily scatter with phonons to higher energies due to the dense spacing of levels in the valence band, conserving energy and allowing the electrons to relax from the QD n=2 to n=1 states [20, 34, 35, 37]. This relaxation mechanism is expected to be quite efficient for the photoexcited carrier density used in these experiments. It is worth noting that intraband-pump, interband-probe experiments on self-assembled QDs that were doped with 4 electrons/dot clearly showed a sequential relaxation between QD levels in the absence of any holes [38]. Our experiments, conducted with approximately the same number of electron-hole pairs per dot, reveal rapid filling of the QD ground state through electron-hole scattering, further demonstrating the impact of this process on energy relaxation in quantum dots.

Figure 3(b) depicts the temporally resolved dynamics at long time delays. The long relaxation at the QD n=1 ground state is due to electron-hole recombination, occurring on a time scale of ~1 ns as determined from curve fits. The aforementioned long-lived DT signal at the QD n=2 excited state is due to state filling, as electron relaxation from the n=2 state will be inhibited once two electrons have filled the n=1 ground state [6, 21]. It is worth mentioning that although the conduction band spacing between the QD n=2 and n=1 states (~38 meV) is larger than the InAs LO phonon energy (~32 meV), electron-hole scattering prevents the observation of a phonon bottleneck [8]. The DT signal at the lowest QW state is also relatively long-lived (~185 ps), which is unexpected as the QD levels can accommodate all 4 photoexcited electron-hole pairs. This may be due to electron-hole scattering, which can scatter electrons into the lowest QW state from the QD n=2 state. However, further investigation is required to isolate the mechanism for the long-lived signal at the lowest QW state. In general, the relatively high photoexcited carrier density in these experiments makes it difficult to extract unambiguous lifetimes for bound-to-bound transitions (i.e., the QD n=2 to n=1 transition).

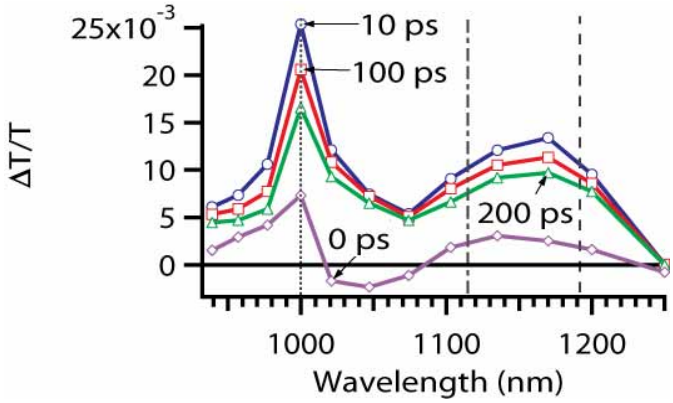

Fig. 4. Differential transmission spectrum taken at 295 K. The approximate positions of the QW n=1, QD n=2, and QD n=1 states are indicated by the dotted, dot-dashed, and dashed lines, respectively.

We now examine the temperature dependence of DWELL carrier dynamics. Differential transmission spectra taken at 295 K are depicted in Fig. 4 for different time delays. The most striking feature of this DT spectrum is that its "camel back" shape stays approximately constant with increasing time delay, contrasting strongly with the 30 K DT spectrum (Fig. 2). This is a strong indication that thermal processes are redistributing the electron and hole populations among the confined QW and QD levels at high temperatures [21, 36]. In addition, the sharp peak at 1000 nm matches well with the QW n=1 transition observed in the PL spectra; its persistence with increasing time delay further indicates that carriers are thermally ejected from QD states into QW states at this temperature.

Figure 5 compares individual time-resolved DT signals at the QW n=1, QD n=2, and QD n=1 transitions at 30 and 295 K, accounting for the red shift in these transitions as determined

#90338 - $15.00 USD Received 30 Nov 2007; revised 18 Dec 2007; accepted 12 Jan 2008; published 15 Jan 2008

from the PL spectra [Figs. 1(b), 1(c)]. As described above, the lack of temperature dependence in the early time dynamics reveals that carrier capture into the QDs is due to Auger scattering, with minimal influence from phonon emission. Carrier relaxation dynamics are quite similar at 295 K for all probe wavelengths; curve fits show that the long time constant at 295 K exhibits relatively little variation (a factor of 2) over the measured wavelength range, unlike at 30 K where it varies by an order of magnitude. This indicates that carriers are both remitted and reabsorbed through thermal processes at room temperature, leading to a nearly energy-independent relaxation of electrons and holes at long times. The DT signal at the QW n=1 state persists for much longer times at 295 K than at 30 K, again due to thermal emission. As at 30 K, the QD n=2 DT signal at 295 K is long-lived (~1.1 ns), supporting the idea that state filling, not a phonon bottleneck, is responsible for this signal. In addition, the similarity between the QD n=1 DT signals indicates that recombination times do not change significantly with temperature in the DWELL heterostructure. Finally, we also measured the differential transmission spectrum at 150 K (not shown); this was very similar to the 30 K DT spectrum, indicating that the physical processes influencing carrier relaxation at 30 K should also apply at 150 K. This also suggests the potential of DWELL-based devices for operating at temperatures at least as high as 150 K; in fact, room temperature operation has recently been demonstrated in a DWELL-based photodetector [39].

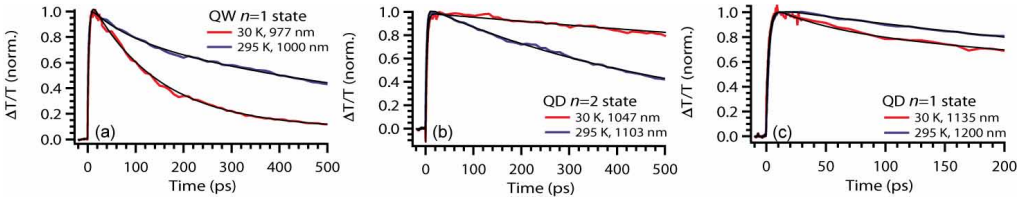

Fig. 5. Normalized time-dependent DT signals at the (a) QW n=1, (b) QD n=2, and (c) QD n=1 states at 30 and 295 K.

3. Conclusion

In conclusion, we have temporally resolved carrier relaxation in a quantum dots-in-a-well heterostructure using differential transmission spectroscopy. We find that electron-electron scattering governs electron capture into the QDs from the QWs, with electron relaxation from the QD n=2 to the QD n=1 state governed by electron-hole scattering at low temperatures. At higher temperatures, thermal emission plays a significant role in the measured dynamics, distributing the electron and hole populations among many adjacent levels. These experiments are a first step towards understanding carrier capture and relaxation across multiple spatial dimensions, with implications for DWELL-based lasers and photodetectors. Future work will focus on measuring ultrafast dynamics at lower carrier densities, directly pumping the excited state to examine gain dynamics, and examining carrier dynamics in different DWELL heterostructures.

Acknowledgments

We sincerely thank S. A. Trugman, G. Jolley, and W. W. Chow for helpful discussions and Tom Vandervelde and Jiayi Shao for assistance with the PL measurements. This work was performed, in part, at the Center for Integrated Nanotechnologies, a U.S. Department of Energy, Office of Basic Energy Sciences user facility. Los Alamos National Laboratory, an affirmative action equal opportunity employer, is operated by Los Alamos National Security, LLC, for the National Nuclear Security Administration of the U. S. Department of Energy under contract DE-AC52-06NA25396. We also acknowledge support from AFRL Contract FA9453-07-C-0171 and NSF Grant ECS-0428756/ ECS-0401154.

#90338 - $15.00 USD Received 30 Nov 2007; revised 18 Dec 2007; accepted 12 Jan 2008; published 15 Jan 2008